Supplementary Information

Target-triggered CRISPR-Cas13a autocatalysis-driven amplification strategy for one-step detection of circadian clock gene

Zhiyuan Feng,[+,a] Yi Xue, [+,a] Yangfang Yun, [+,a], Zheng Liu, [a] and Jingjing Zhang [a]

[a] *State Key Laboratory of Analytical Chemistry for Life Science, School of Chemistry and Chemical Engineering, Chemistry and Biomedicine Innovation Center (ChemBIC), Nanjing University, Nanjing 210023, China*

\+ *These authors contributed equally to this work*

** Corresponding Author: Prof. JingJing Zhang*
Email: jing15209791@nju.edu.cn

Section 1.

Expression and purification of Cas13a protein

We followed a previously published protocol to obtain purified LbuCas13a with some modifications.[1] Briefly, the plasmid p2CT-His-MBP-Lbuc2c2_WT was transformed into *E. coli Rosetta* (DE3), and the cells were cultured in Luria-Bertani (LB) medium with 100 μg/mL ampicillin (Macklin) at 37 ℃. When OD_{600} reaches 0.6, the cells were induced overnight at 16 °C with 0.5 mM IPTG, followed by centrifugation at 8000 rpm for 10 min at 4 ℃. Bacteriophage were then added to the lysis buffer (20mM Tris-HCl,1M NaCl，20mM imidazole, pH=7.5) with 1 mM PMSF and 0.2mg/mL lysozyme in 4℃ for overnight resuspension. The protein were extracted by sonication, the centrifugal supernatant collected by centrifugation for 40min at 4℃, 10000rpm. Then the supernatant was filtered through a 0.45μm filter membrane and incubated with Ni-NTA metal affinity column for 1 hour at 4℃.The bound protein were washed with binding buffer (contain 20 mM imidazole)and eluted with elution buffer(contain 250 mM imidazole). To remove His-MBP tag, TEV protease with His Tag was incubated with elution solution according to the manufacturer's instructions. Purified LbuCas13a was reloaded onto a pre-equilibrated Ni-NTA column to removed His-MBP tag. After all the concentration were concentrated by 30KDa molecular mass cut-off concentrators (Millipore) with protein exchange buffer (20mM Tris-HCl, 600mM NaCl, pH=7.5) were concentrated to 20 μM and transferred into storage buffer. The protein was stored at –20 °C for later use.

***In vitro* transcription and purification of crRNA**

To prepare crRNA, the DNA oligos (Table S2) were appended with the T7 promoter sequence at the 5' end and dissolved in DEPC-treated water. The annealing process was performed by heating the solution to 95°C for 5 minutes and then gradually cooling it down to 25°C with a 0.1°C/s ramp. This was done to conform the dsDNA templates with double-stranded T7 promoter sequences. *In vitro* transcription was carried out using the Hyper Scribe T7 High Yield RNA Synthesis Kit (K1047, APEXBIO) as per the manufacturer's instructions. To remove the DNA templates, DNase I without RNase (Sangon) was incubated with the RNA product at 37°C for 30 minutes. The purified crRNA was obtained using the Monarch RNA Cleanup Kit (T2040S, New England Biolabs) according to the manufacturer's instructions. The concentration of all crRNA

was determined by a Nanodrop One (ThermoFisher) and stored at -80°C. The list of all crRNA used in this work is given in Table S2.

3D structure prediction and MD simulation of crRNA-BMAL1

According to the nucleic sequences of LbuCas13a crRNA (Figure 1A) and WT/mutated BMAL1 (Perfect/SM-4, SM-5) (Figure 3A), the second structures of crRNA1-WT/mutated BMAL1 complex were predicted by the RNAfold web server (http://rna.tbi.univie.ac.at//cgi-bin/RNAWebSuite/RNAfold.cgi). Then, the 3D structures of RNA complex model were calculated using the FARFAR2 protocol [2] in the Rosetta software, the conformation with the highest absolute score was selected from the 10 predicted 3D models as the studied structure.

To study the effect of mutations in BMAL1 on crRNA1, we adopted molecular dynamics (MD) simulation for complexes of crRNA1 with WT/mutated BMAL1 (Perfect/SM-4, SM-5), respectively by AMBER 2022 software [3]. The *ff99OL3* force field [4-5] was applied on the RNA. Every system was solvated in a periodic TIP3P octahedron box [6]. The minimum distance from the complex atom of aptamer-streptavidin to the edge of the box was set to be 10.0 Å. Corresponding number of counter-ions (Na^+) were added to neutralize the charge. After minimization and system warming, the MD simulations of three study systems were performed in the NVT ensemble for 10 ns, respectively. Finally, the trajectory analysis was performed by the CPPTRAJ program [7] integrated in the AMBER software, the root-mean-square deviation (RMSD) value of backbone atoms relative to the initial conformation were computed (Figure S6A) .The last frame of the MD simulation process was extracted as their final conformation, respectively (Figure S6B).

Construction of LbuCas13a-crRNA1-target RNA ternary complexes

Because the crRNA1' repeat region and Cas13a in this work are identical to the reported crystal structure of LbuCas13a-crRNA-target RNA ternary complex (PDB ID: 5XWP)[8], with reference to the RNA binding sites of 5XWP, the ternary complexes were obtained by manually docking the crRNA1-WT/mutated BMAL1 binary structures obtained from MD simulation into the channel of the protein with reference to binding site, keeping the repeat binding mode of crRNA1 unchanged. The ternary complexes and molecular interaction diagrams were drawn by PyMOL (Schrödinger, LLC) and VMD software [9].

Table S1. The sequences of RNA in this work

Name	Information of the RNA sequences (5'-3')
iRNA-1	ACUACAACUGUUUUUUUCGUAUAUCAUA-BHQ1
iRNA-2	CUGUAGAGUGUUUUUUUCAUAACGAUC
iRNA-1-blank	ACUACAACUGUUUUUUUCGUAUAUCAUA
RNA intermediate	FAM-UAUGAUAUACGCAGUUGUAGUGAUCGUUAUGCACUCUACAG
mBMAL1	GGUCGAAUGAUCGCGGAGGAAAUCAUGGAAAUCCACA
crRNA1	GGACCACCCCAAAAAUGAAGGGGACUAAAACUCCAUGAUUUCCUCC GCGAU
crRNA2	GGACCACCCCAAAAAUGAAGGGGACUAAAACUGCAUAACGAUCACUA CAAC
FQ-reporter	FAM-UUUUUU-BHQ1
MM-1	AUCGCGGAGGAAAUCAUGGG
MM-2	AUCGCGGAGGAAAUCAUGUA
MM-3	AUCGCGGAGGAAAUCAUCGA
MM-4	AUCGCGGAGGAAAUCAAGGA
MM-5	AUCGCGGAGGAAAUCGUGGA
MM-6	AUCGCGGAGGAAAUUAUGGA
MM-7	AUCGCGGAGGAAACCAUGGA
MM-8	AUCGCGGAGGAAGUCAUGGA
MM-9	AUCGCGGAGGAUAUCAUGGA
MM-10	AUCGCGGAGGCAAUCAUGGA

Table S2. The DNA sequence in this work

Name	Information of the DNA sequences (5'-3')
crRNA1_F	TAATACGACTCACTATAGGACCACCCCAAAAATGAAGGGG
	ACTAAAACTCCAUGATTTCCTCCGCGAT
crRNA1_R	ATCGCGGAGGAAATCATGGAGTTTTAGTCCCCTTCATTTT
	TGGGGTGGTCCTATAGTGAGTCGTATTA
crRNA2_F	TAATACGACTCACTATAGGACCACCCCAAAAATGAAGGGG
	ACTAAACTGCATACGATCACTCAAC
crRNA2_R	GTTGAGTGATCGTATGCAGTTTAGTCCCCTTCATTTTTGG
	GGTGGTCCTATAGTGAGTCGTATTA
BMAL1-pF	TCCAGTCTTGGCATCAATGAGT
BMAL1-pR	CCTAATTCTCAGGGCAGCAGAT
Actin-F	ACCAACTGGGACGACATGGAGAAA
Actin-R	ATAGCACAGCCTGGATAGCAACG

Table S3. Different detection ranges and limits for cleavage substrates

Substrate	Linear range	LOD
F-Q probe	10 fM-1 nM	2.9 fM
TSRP probe	1 pM-1 nM	0.7 pM
TSRP probe (plus crRNA2 RNP)	100 aM-1 nM	4.6 aM

Table. S4. Comparison of recently developed CRISPR methods on detection of RNA

Method	System name	Target	LOD	specificity	Ref.
Electrochemilum-inescence	PECL-CRISPR	miR-17	1 aM	Medium	10
Fluorescence	PCDetection	miRNA-143	50 fM	High	11
Colorimetric	vCas	miR-10b	1 fM	High	12
Colorimetric	HECA	miRNA-143	1 fM	Medium	13
Colorimetric	CESSAT	SARS-CoV-2 RNA	1 copy/μL	High	14
Fluorescence	CRISPR-ACC	mBMAL1	4.6 aM	Medium	This work

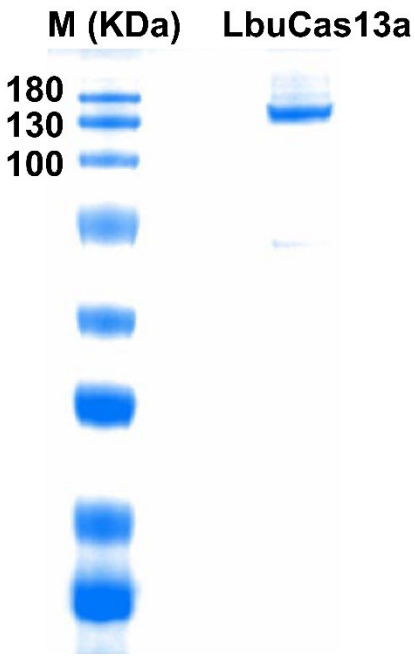

Figure S1. Analysis of the expression of LbuCas13a protein by SDS-PAGE (10%).

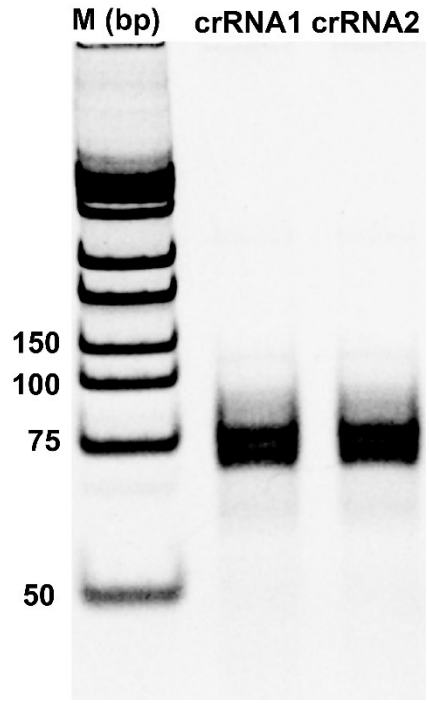

Figure S2. Analysis of the crRNA by denaturing 8 M urea/10% polyacrylamide gel (Urea-PAGE). Marker: low molecular weight DNA ladder (25-500 bp).

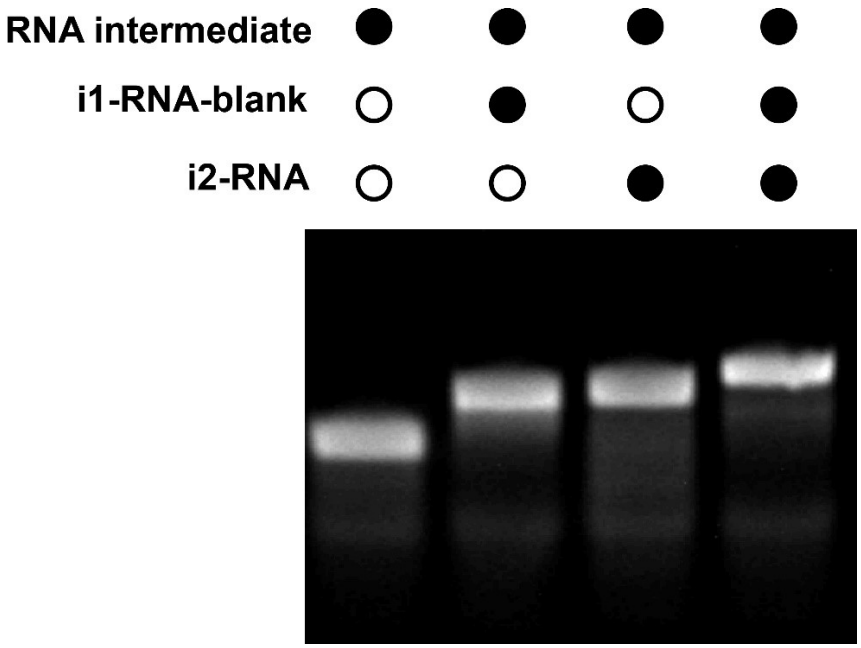

Figure S3. Analysis of the TSRP assembly process with 12% nature PAGE.

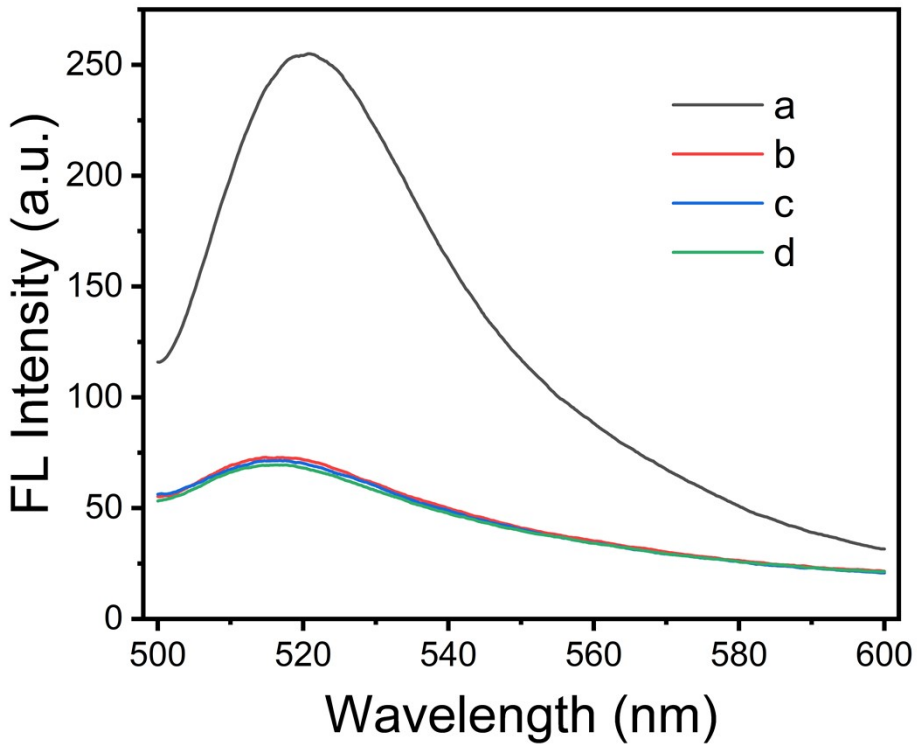

Figure S4. Capability of signal enhancement through CRISPR-ACC coupled with TSRP. (a) Cas13a/crRNA1 + TSRP + BMAL1 (1 nM); (b) Cas13a/crRNA1 + TSRP; (c) Cas13a + BMAL1 (1 nM) + TSRP; (d) TSRP only. The concentrations of Cas13a, crRNA1, and TSRP is 20 nM, 20 nM, and 200 nM, respectively.

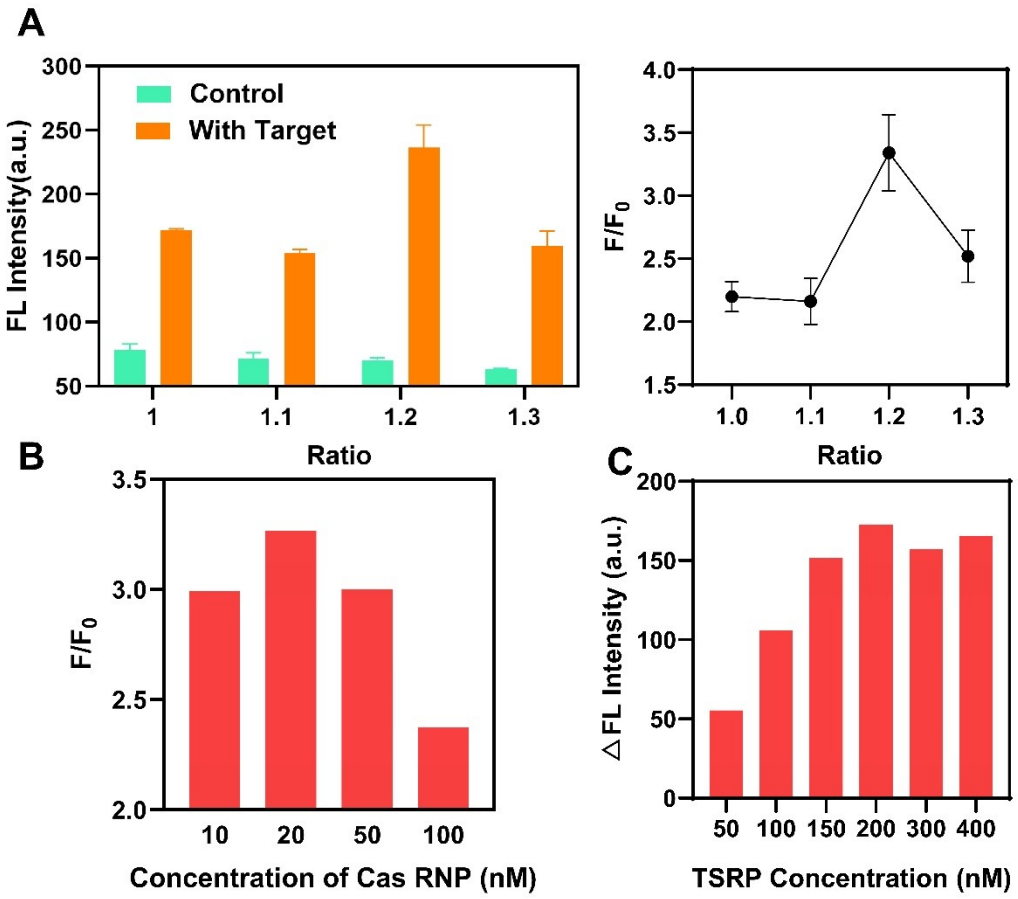

Figure S5. Optimization of ACC system. (A) Effect of the ratio of [i-RNAs]/ [RNA intermediate] on the signal and background fluorescence. LbuCas13a/crRNA: 20 nM; TSRP: 200 nM. The two iRNAs are used in equivalate molar amount to prepare TSRP. Optimize Cas protein concentration (B) and TSRP substrate concentration (C).

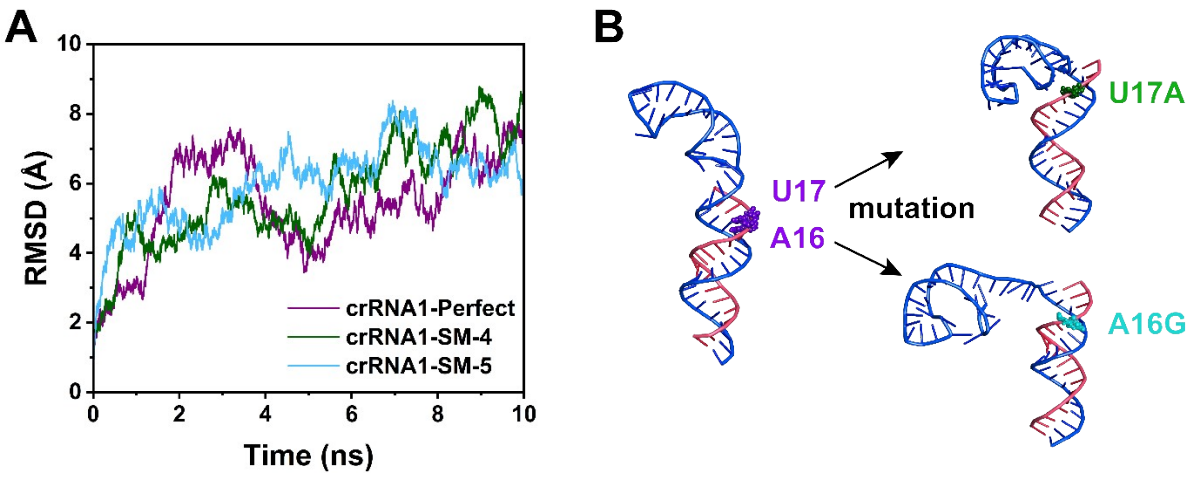

Figure S6. MD simulations of crRNA1-BMAL1 (Perfect/SM-4/SM-5) binary complexes. A: The RMSD plots of crRNA1-BMAL1 (Perfect/SM-4/SM-5) complex backbone atoms over simulation times. B: The final conformations of RNA binary complex after MD simulations. The mutated sites are highlighted as colored balls.

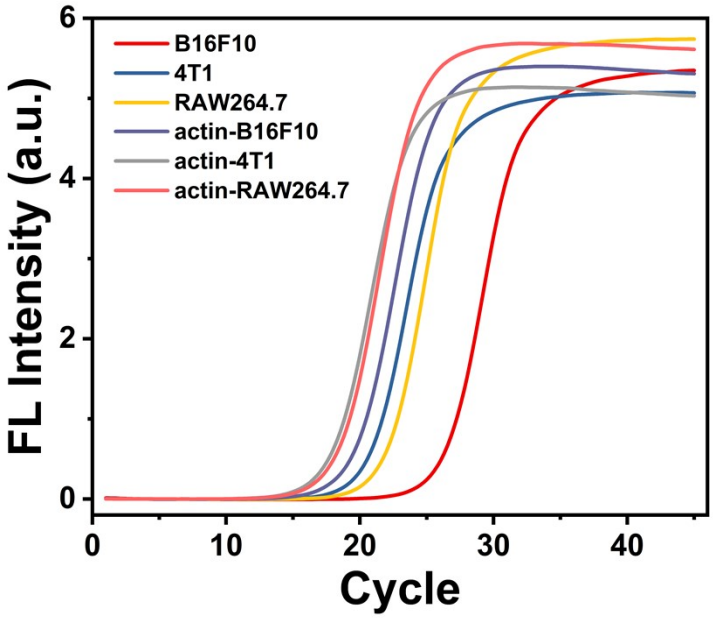

Figure S7. RT-PCR fluorescence kinetic curves for total RNAs extracted from different cells.

Table S5. RT-PCR results of different cells

Note	Ct BAML1	Ct β-actin	−ΔΔCt	Fold change
B16F10-1	24.79	17.82	3.07	0.11908
4T1-1	19.27	16.19	-0.82	1.765406
RAW264.7-1	20.43	16.53	-	1
B16F10-2	24.73	17.96	2.9	0.133972
4T1-2	19.29	16.29	-0.87	1.827663
RAW264.7-2	20.47	16.60	-	1
B16F10-3	24.74	17.79	3.06	0.119908
4T1-3	19.26	16.18	-0.81	1.753211
RAW264.7-3	20.42	16.53	-	1

Reference

[1] J. S. Gootenberg, O. O. Abudayyeh, M. J. Kellner, J. Joung, J. J. Collins, F. Zhang, **Science**,2018, 360: 439-444

[2] Watkins, A. M.; Rangan, R.; Das, R. "FARFAR2: Improved de novo Rosetta prediction of complex global RNA folds." **Structure**, 2020, 28: 963–976.

[3] Case, D. A.; Aktulga, H. M.; Belfon, K.; Ben-Shalom, I. Y.; Berryman, J. T.; Brozell, S.R.; Cerutti, D. S.; Cheatham,T. E.; Cisneros, G.A.; Cruzeiro, V. W. D.; Darden, T.A.; Duke, R. E.; Giambasu, G.; Gilson, M. K.; Gohlke, H.; Goetz, A. W.; Harris, R.; Izadi, S.; Izmailov, S.A.; Kasavajhala, K., et al,; **Amber 2022**, University of California, San Francisco, 2022.

[4] A. Perez, I. Marchan, D. Svozil, et al. Refinement of the AMBER Force Field for Nucleic Acids: Improving the Description of alpha/gamma Conformers. **Biophys J**, 2007, 92, 3817–3829.

[5] M. Zgarbova, M. Otyepka, J. Sponer, et al. Nucleic Acids Force Field Based on Reference Quantum Chemical Calculations of Glycosidic Torsion Profiles. **J Chem Theory Comput**, 2011, 7, 2886–2902.

[6] Jorgensen WL, Chandrasekhar J, Madura JD. Comparison of simple potential functions for simulating liquid water. **J Chem Phys**, 1983, 79: 926-935.

[7] D. R. Roe and T. E. Cheatham III, PTRAJ and CPPTRAJ: Software for processing and analysis of molecular dynamics trajectory data, **J Chem Theory Comput**, 2013, 9, 3084.

[8] Liu L, Li X, Ma J, Li Z, You L, Wang J, Wang M, Zhang X, Wang Y. The Molecular Architecture for RNA-Guided RNA Cleavage by Cas13a. **Cell**. 2017, 170: 714-726.

[9] Humphrey W, Dalke A, Schulten K. VMD: visual molecular dynamics. **J Mol Graph.** 1996,14: 33-8, 27-8.

[10]. T. Zhou, R. Huang, M. Huang, J. Shen, Y. Shan, D. Xing, **Adv. Sci.** 2020, 7, 1903661.

[11] M. Zhong, K. Chen, W. Sun, X. Li, S. Huang, Q. Meng, B. Sun, X. Huang, X. Wang, X. Ma, P. Ma, **Biosens. Bioelectron.** 2022, 214, 114497.

[12] T. Zhou, M. Huang, J. Lin, R. Huang, D. Xing, **Anal. Chem.** 2021, 93, 4, 2038–2044

[13] W. Jiang, Z. Chen, J. Lu, X. Ren, Y. Ma, **Talanta**.2023, 251, 123784.

[14] Y. Wang, H. Chen, H. Gao, H. Wei, Y. Wang, K. Mu, L. Liu, E. Dai, Z. Rong, S. Wang, **Biosens. Bioelectron.** 2023, 229, 115238.